Ab initio determination of the electronic structure of beryllium-, aluminum-, and magnesium-nitrides: A comparative study

Ma. Guadalupe Moreno Armenta
Programa de Posgrado en Física de Materiales del Centro de Investigación Científica y de Educación Superior de Ensenada, Km. 107 Carretera Tijuana-Ensenada, Ensenada, B.C. Mexico

Armando Reyes-Serrato* and Miguel Avalos Borja
Centro de Ciencias de la Materia Condensada de la UNAM, Apartado Postal 2681, Ensenada, Baja California, 22800 Mexico
(Received 19 July 1999; revised manuscript received 12 April 2000)

We have investigated the electronic properties, in different crystal phases of the Be_3N_2 (alpha and beta), AlN (wurtzite and zinc blende) and Mg_3N_2, compounds within an all-electron *ab initio* linear combination of atomic orbitals self-consistent-field-Hartree-Fock approximation with *a posteriori* density-functional correction. Results include lattice parameters, bulk moduli and its derivative, band structure, density-of-states, charge density, and Mulliken population analysis. We also presented aluminum nitride band calculations obtained by various methods, showing that our results lie within previously calculated values and in good agreement with experimental data. Addionally the alpha phase of beryllium nitride, presents a direct band gap of 4.47 eV and might have application in blue/UV light-emitting diodes and lasers.

I. INTRODUCTION

Considerable interest has arisen in the wide band gap Group-III-V nitrides as possible candidates for applications of blue/ultraviolet (UV) light-emitting diodes and laser diodes.[1,2] The demonstration of stimulated emission in the blue region has served to further increase awareness of the potential of nitride based devices.[3,4] These Group-III-V compounds, has been extensively studied[5] because they show in addition to wide band gap, high-thermal conductivity and large bulk moduli making them promising materials.

In the area of optoelectronics, they fulfill the need for materials emitting light of short wavelengths. Blue light emission is needed for full color displays and UV emission is optimal for optical communications because of its higher information density.[6,7]

As far as the gaps themselves are concerned, nitrides seem to be leading with gaps as high as 6.28 eV for AlN.[8] Furthermore, the wurtzite compounds AlN, GaN, and InN all have direct gaps. This is an important advantage for optoelectronic light-emitting devices.

In this paper we studied the electronic properties of Be_3N_2 (alpha and beta), AlN (wurtzite and zinc blende) and Mg_3N_2. In our search, we did not find any papers about electronic properties of the α-beryllium and magnesium nitride, thus to our knowledge, this is the first-principles determination of the electronic structure on these compounds. We performed all-electron, *ab initio* calculations using Hartree-Fock with linear combination of atomic orbitals method (LCAO), *a posteriori* density-functional (DFT) corrections.

Considerations about hardness, melting point, and ionic potential (rate charge to radius), suggests that beryllium is an exception of the Group-IIA family, and it is more like the aluminum family.[9] We can compare the aluminum and beryllium nitride characteristics, studying their electronic structure.

We focus our attention on differences in the band gap between these compounds as well as on the bonding properties of the beryllium, aluminum, and magnesium cations, related to the ionic/covalent character of the bonds in the considered compounds.

The calculations presented in this paper were motivated by the search of new materials with relevant technological characteristics. This paper is organized as follows: in Sec. II we give a brief description of the calculation method, in Sec. III we report results and discussion of the structural and electronic properties, and Sec. IV contains the conclusions.

II. CALCULATION METHOD

A. Crystal Structure

The beryllium nitride has two known phases: alpha and beta. The alpha phase is a cubic bcc structure like anti-Mn_2O_3 (bixbyte),[10,11] which is stable between 20–1200 °C (Refs. 12 and 13) and at temperatures over 1400 °C changes to a hexagonal structure, which is the beta phase.[14] The alpha beryllium-, and magnesium-nitride crystallize in the bixbyte structure,[15] the unit cell is formed by 80 atoms [Fig. 1(a)], with lattice parameters $a=8.145$ Å and 9.96 Å, respectively,[16] and the space group is Ia3 (206).[17] The primitive cell has 40 atoms, 24 Be (Mg) and 16 N, with a total of 208 (400) electrons. The β-Be_3N_2 phase [Fig. 1(b)], has parameters $a=2.8413$ Å and $c=9.693$ Å and the space group is P6/mmc(194).[15] The primitive cell has 10 atoms, 6 Be and 4 N, with a total of 52 electrons per cell. AlN has a wurtzite-type structure [Fig. 1(c)] with $P6_3mc$ (186), $a=3.111$ Å and $c=4.978$ Å.[15] The primitive cell has 4 atoms, 2 Al and 2 N, with a total of 40 electrons per cell. The zinc-blende phase of AlN has a F43m (216) space group and $a=4.365$ Å [Fig. 1(d)]. The primitive cell has 2 atoms, 1 Al and 1 N, with a total of 20 electrons per cell.

Calculations were performed within all-electron *ab initio* self-consistent field (SCF) periodic Hartree-Fock (HF)

 ©2000 The American Physical Society

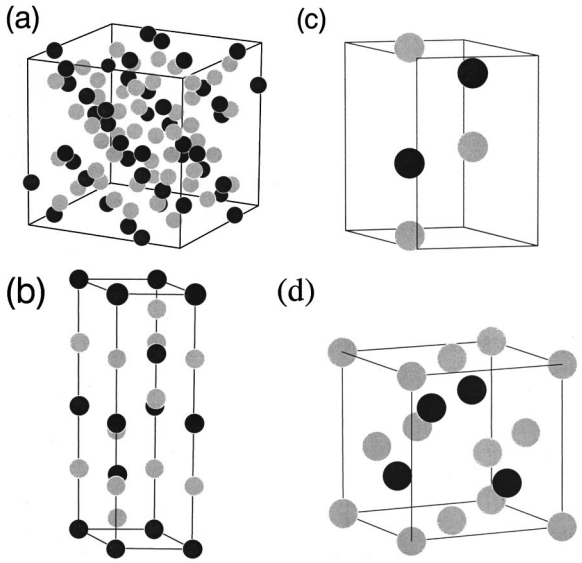

FIG. 1. Unit cell of (a) α-Be_3N_2 and Mg_3N_2, (b) β-Be_3N_2, (c) AlN (wurtzite), and (d) AlN (zinc blende). Gray balls represent cations atoms and black balls nitrogen atoms.

LCAO procedure as implemented in CRYSTAL 95.[18] *A posteriori* density-functional corrections to the Hartree-Fock results for the total energy have been included, with the correlation functional proposed by Perdew, Zunger, and Becke (PZB).[19] A description of the periodic HF-LCAO-SCF computational scheme in this program has been previously described[20] and will be omitted here.

Regarding the basis set in crystal, the Bloch functions are constructed from localized atomic orbitals, which in turn are linear combinations of Gaussian-type functions, that are the product of a Gaussian and a real solid spherical harmonic. As in the molecular Hartree-Fock calculations, the results can be quite sensitive to the choice of the basic set.[21] For the present calculations the *all-electron* basis set 6-21G for Be, Al, Mg, and N have been used. They contain 9 functions for Be and N (a contraction of 6, 2, and 1 Gaussian type function for the $1s$, $2sp$, and $3sp$ shells) from tables 4.39.1 and 7.77.1, respectively.[22] and 15 for Mg and Al (6-6-2-1 contraction for $1s$, $2sp$, $3sp$, $4sp$ shells) from tables 12.16.1 and 13.19.1 respectively.[22] The addition of *d*-type polarization functions on all atoms give the 6-21G* basis set. In order to make the basis set more adequate for crystal calculations the last exponent of each base set was reoptimized using the values proposed in Refs. 18, 23, and 24, see Table I.

The level of numerical approximation, in evaluating the Coulomb and exchange series appearing in the SCF equations for periodics systems, is controlled by five tolerance parameters.[25] These are related to estimates of overlap or penetration for integral of Gaussian function on a different center, which define cutoff limits for series summation. The values used in the present calculations were 10^{-6},10^{-6},10^{-6},10^{-6}, and 10^{-8}.

TABLE I. Exponents for the most diffuse Gaussian functions adopted for the present paper.

Atoms	α_{sp} 6-21G	α_{sp} 6-21G*	α_{d} 6-21G*
Be	0.2	0.2	0.8
Al	0.3	0.15	0.51
Mg	0.3	0.2	0.178
N	0.3	0.28	0.8

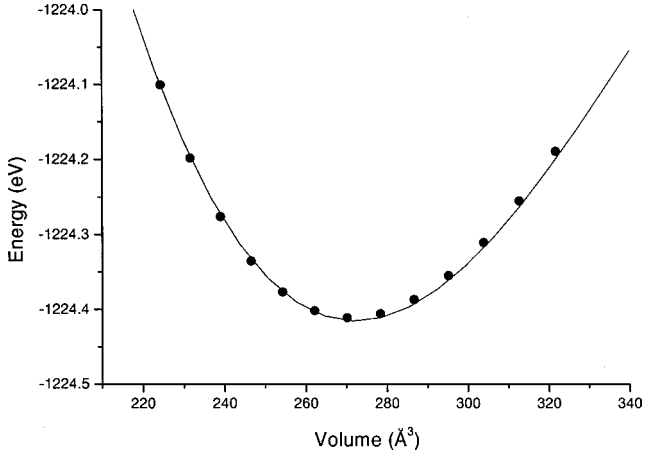

FIG. 2. Total energy *vs* volume for α-Be_3N_2. Continuous line represents fit with Murnaghan's state equation.

III. RESULTS AND DISCUSSION

A. Structural properties

The ground-state properties of the nitrides structures are obtained by minimization of the total energy with respect to the unit-cell volume (V). A uniform compression and expansion of the lattice, with the relative positions within the unit cell held constant, were used to make isotropical variation of the cell volume. In Fig. 2, we show the calculated total energy for α-Be_3N_2, as a function of the cell volume. The $E(V)$ curve was fitted by the Murnaghan equation-of-state[26] by using the Levenberg-Marquardt method[27] to obtain the lattice parameters of the equilibrium structure, and to evaluate the bulk modulus (B). The $E(V)$s curves for the rest of the compounds are not shown because they are all similar, but the results are summarized in Table II. As we can see, (Table II) the lattice parameters are in excellent agreement with the experimental values for all nitride structures. Our results of bulk modulus for the AlN wurtzite phase differ by 11% with largest experimental data; this discrepancy may be due to the fact that in transformation procedures an ideal wurtzite structure is assumed, neglecting the relaxation of the lattice constant ratio c/a and the internal parameter u from their ideal values.

B. Band structure and density-of-states

The Hartree-Fock method for periodic systems usually overestimate the optical gap and bandwidth because they do not take into account electronic correlation. In order to make adjustments we perform *a posteriori* DFT calculations. Figure 3 shows the calculated band structure, using *all electron* basis set 6-21G*. Figure 3(a) shows the band structure for α-Be_3N_2 (usual symmetry reference points for bcc are indicated). The central Brillouin-zone gamma point (Γ) exhibits a direct band gap of 4.28 eV. The valence band is separated in two regions by a 6.057 eV band gap, the upper bandwidth is 7.49 eV, while the lower bandwidth is 3.11 eV. For optical

TABLE II. Lattice parameters, bulk modulus (B), and its derivative (B'), and total energy per cell, obtained by mean of *all-electron* Hartree-Fock calculations with 6-21G basis, for AlN, Be_3N_2, and Mg_3N_2 Experimental results are included for comparison.

		a(Å)	c(Å)	B (Mbar)	B'	E_0 a.u./cell
α-Be_3N_2	present calc.	8.155		2.57	2.93	−1224.411
	exp. [a]	8.145				
β-Be_3N_2	present calc.	2.847	9.720	2.36	3.60	−306.009
	calc. [b]	2.842	9.695	2.39	3.29	−306.139
	exp. [c]	2.841	9.693			
AlN	present calc.	3.082	4.935	2.69	3.49	−576.257
(wurtzite)	calc. [d]	3.082	4.946	2.15	3.6	
	calc [e]	3.129	4.988	1.95	3.74	
	exp. [f]	3.111	4.978	2.08[g]		
	exp. [h]			2.37		
AlN	present calc.	4.336		2.68	3.30	−289.125
(zinc blende)	calc. [d]	4.337		2.14	3.3	
	exp. [g]	4.365				
Mg_3N_2	present calc.	9.858		1.65	3.66	−5662.67
	exp. [a]	9.96				

[a]Reference 16.
[b]Reference 23.
[c]Reference 28.
[d]Reference 29.
[e]Reference 30.
[f]Reference 15.
[g]Reference 31.
[h]Reference 32.

applications, not only the magnitude of the gap is important but whether or not it is a direct or indirect gap is very important. The only semiconductor with a direct band gap larger than 5 eV known to date, seems to be wurtzite AlN (6.28 eV). There are other semiconductors with direct band gap, but not greater that 3.76 eV.[33] Therefore, a material with a direct gap well into the ultraviolet (UV) range would be of great interest. The band gap calculated for the α-Be_3N_2 is 4.28 eV or (4.47 eV without polarization function), locating it in the UV range.

In Fig. 3(b), we show the band structure for beryllium nitride hexagonal phase, the valence band also is separated in two regions by an 5.85 eV gap. The bandwidth of the p_N band is strongly correlated to the distance between the nearest nitrogen atoms (D_{N-N}).[34] The difference between the two bandwidths (7.66 eV for β-Be_3N_2 and 7.44 eV for α-Be_3N_2) may be attributed to the close D_{N-N} values in the two structures (2.84 Å and 2.71 Å, respectively). This difference is smaller by 0.22 eV. In compounds with marked ionic character this difference is as high as 1–2 eV. On the other hand, the p derived valence-band widths of 7.66 eV and 7.44 eV indicate that the wave function ionic sites are less localized compared with more ionic compounds as NaCl and KCl.[35]

The principal difference lies in the evaluation of the optical gap, where the beta phase present an indirect band gap at Γ-M and the alpha phase present a direct band gap at Γ. This effect is also observed in the widely used Group-III-V semiconductors.

AlN in the wurtzite phase, [Fig. 3(c)] shown a direct band gap at Γ point of 5.25 eV (or 5.47 eV without polarization function), this value is close to the experimental value of 6.28 eV. The calculated width of the total valence band (15.32 eV) agrees well with the value of 16 eV estimated from photoemission and x-ray emission spectroscopic data of Gautier *et al.*[36] As for the upper valence zone, the calculated and experimental values are 5.93 eV an 6.0 eV, respectively.

The band structure from aluminum nitride zinc-blende phase is shown in Fig. 3(d). It has a valence band split into two sections by a 6.89 eV gap, the upper width with a value of 5.63 eV and a lower width of 2.49 eV. Comparing both phases (wurtzite and zinc blende), we observed that, D_{N-N} presents close values, 3.07 Å and 3.09 Å, respectively, and in consequence the upper valence-band widths are very similar. With respect to the optical gap, while wurtzite is direct, AlN zinc blende is indirect (Γ-X).

In Fig. 3(e) the band structure of Mg_3N_2 is displayed and we note that the band gap is indirect occurring between Γ (the valence-band maximum) and a point along the ΓN line (the conduction-band minimum). The indirect band-gap value is 2.25 eV while the direct is 2.26 eV. The occupied bands fall into two groups separated by a 7.94 eV band gap, the upper valence band has a width of 3.89 eV and the lower valence band a width of 1.29 eV.

In Table III we summarize our results for the band structure and those from literature. We show that our results for AlN lie within previously calculated values and in good agreement with experimental data (Table III).

Comparing the nitrides structures in the paper, we see that for the compounds with hexagonal symmetry, the top of the valence band (Γ point) is split into two levels, in contrast to the cubic structures where the top of the valence band is triply degenerate.

AlN compounds (zinc blende and wurtzite), have a coordination number (N_C)=4 and Group-II-nitrides Be_3N_2 and Mg_3N_2 (bixbyte) have N_C=4 and N_C=6 in the cation and anion, respectively. In the fourfold coordinated sites the s-p valence electrons are fully hybridized and form sp^3 valence orbitals. In the sixfold coordinated sites, the s and p^3 bonds

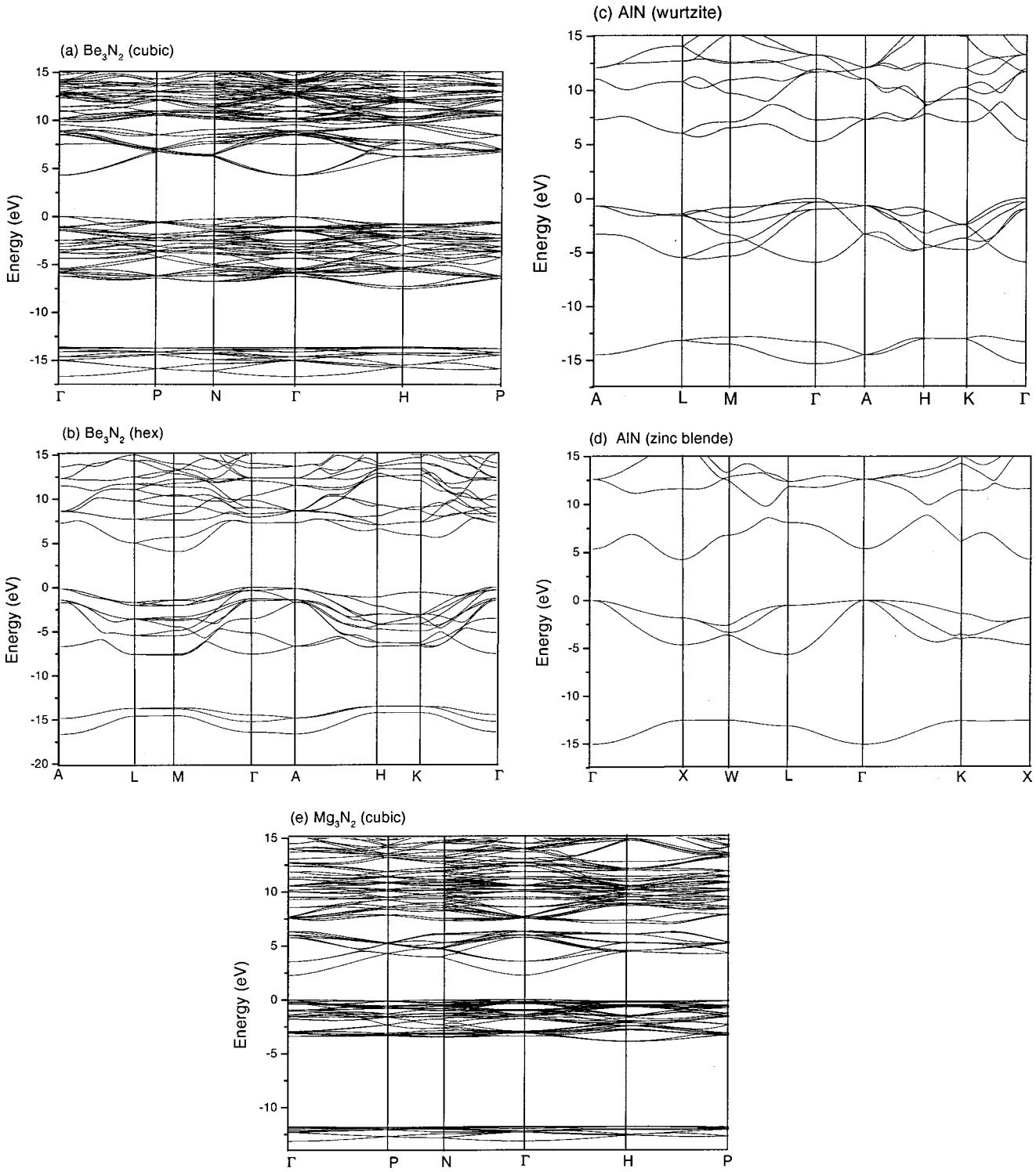

FIG. 3. Band structure for the nitrides under study, (a) α-Be_3N_2, (b) β-Be_3N_2, (c) AlN (wurtzite), (d) AlN (zinc blende), and (e) Mg_3N_2. The zero in energy corresponds to valence-band top.

do not hybridize and the dominant valence orbitals are the p_x, p_y, and p_z. The bandwidths of the *s* and *p* band become, in the ionic limit, small compared to the anion *s*-*p* energy difference.

We observed that Be and Al nitrides show similars properties such as: ionic/covalent character, optical gap, and valence bandwidth, in spite of different structures and differences in the coordination numbers. That confirms that beryllium is like aluminum.

The width in the antisymmetric gap (Table III) shows that the variation in Mg_3N_2 is the largest and that the variation in Be_3N_2 is the smallest for both phases; this gap is related to the ionicity of the semiconductor.[41]

We noticed that when we use the 6-21G* basis set, this leads to a reduction of the band gap and valence bandwidths, as is evident from the values on Table III. The main effect of including the *d* states is to put strength into the upper valence band and lower the conduction band.

TABLE III. Results of band calculations for AlN (wurtzite), AlN (zinc blende), α-Be_3N_2, β-Be_3N_2, and Mg_3N_2, accomplished with different methods, is shown the value of the band-gap minimal (E_g), the valency bandwidth, and antisymmetric gap (E_A). Methods include pseudopotencial plane-wave (PPPW), local-density approximation (LDA), linear combination of atomic orbitals (LCAO), generalized density functional theory in the local-density approximation (GDFT/LDA), Hartree-Fock (HF), Hartree-Fock with correlation functional proposed by Perdew-Zunger and Becke (HF+PZB). Present values were obtained using basis set 6-21G and 6-21G*. Experimental values are included for comparison.

Compound	Calculation		$E_g(eV)$	Valence	bandwidth	E_A
α-Be_3N_2	Present paper		Direct (Γ)	Upper	Total	
	HF		12.69			
	HF+PZB (6-21G)		4.47	7.58	16.75	6.02
	HF+PZB (6-21G*)		4.28	7.49	16.65	6.06
β-Be_3N_2	Present paper		Indirect ($\Gamma-M$)			
	HF		12.36			
	HF+PZB (6-21G)		4.46	7.79	16.87	5.80
	HF+PZB (6-21G*)		4.05	7.66	16.77	5.85
AlN	Present paper		Direct (Γ)			
(wurtzite)	HF		14.40			
	HF+PZB (6-21G)		5.47	6.28	15.64	6.74
	HF+PZB (6-21G*)		5.25	5.93	15.32	6.86
		HF [a]	14.36	8.27		
		PPPW [b]	4.74			
		LCAO [c]	4.44			
		GDFT/LDA [d]	6.01			
		LDA [e]	3.9	6.10	15.20	6.3
		GW [e]	5.8	6.90	17.40	7.7
		Experimental [f]	6.28	6.00	16.00	
AlN	Present paper		Indirect ($\Gamma-X$)			
(zinc blende)	HF		13.19			
	HF+PZB (6-21G)		4.45	6.08	15.41	6.80
	HF+PZB(6-21G*)		4.26	5.63	15.01	6.89
		LDA [e]	3.2	6.00	15.10	6.3
		GW [e]	4.9	6.70	17.00	7.6
Mg_3N_2 cubic	Present paper		Indirect ($\Gamma-N$)			
	HF+PZB (6-21G)		2.06	4.21	13.37	7.74
	HF+PZB (6-21G*)		2.25	3.89	13.12	7.94

[a]Reference 24.
[b]Reference 37.
[c]Reference 38.
[d]Reference 39.
[e]Reference 40.
[f]Reference 8.

The calculated total density-of-states and its orbital-projected contributions for nitrides are displayed in Fig. 4. The general features of these diagrams, show that they are similar among them. The valence band is split by the so-called ionicity gap in two subbands: the upper one lying just below in the top valence band, is essentially dominated by the nitrogen $2p$ states, with a minor presence of p and s [Be, Al] or s, p, and d [Mg] states and the lowest one is formed by the $2s$ levels from nitrogen, with a negligible contribution of s [Be, Al, Mg] orbitals. While the bottom of the conduction band is due to the Be, Al, or Mg, s and p orbitals.

The contribution of the d-type polarization function to the valence band is negligible, while their participation in the conduction band is more important, especially for Al and Mg atoms.

C. Electron density and Mulliken population analysis

The electron probability distribution function $\rho(r)$, is a three-dimensional function defined such that $\rho(r)dr$ is the probability of finding an electron in a small volume element,

$$\rho(r)=\sum_{\mu}^{N}\sum_{\nu}^{N} P_{\mu\nu}\Phi_{\mu}\Phi_{\nu}, \tag{1}$$

where $P_{\mu\nu}$ are elements of the density matrix and $\Phi\mu,\Phi\nu$ represent basis functions. It is desirable to allocate the electrons in some fractional manner among the various parts of a molecule (atoms, bonds, etc.). Suggestions about how to do this, starting from the density matrix, were made by Mulliken.[42] Collectively they now constitute the topic of Mulliken population analysis. Integration of Eq. (1) leads to

$$\int \rho(r)d\tau=\sum_{\mu}^{N}\sum_{\nu}^{N} P_{\mu\nu}\int \Phi_{\mu}\Phi_{\nu}d\tau=\sum_{\mu}^{N}\sum_{\nu}^{N} S_{\mu\nu}P_{\mu\nu}=n, \tag{2}$$

where $S_{\mu\nu}$ is the overlap matrix. The sum of nondiagonal components of Eq. (2) is referred to as overlap population[43] (see Table IV).

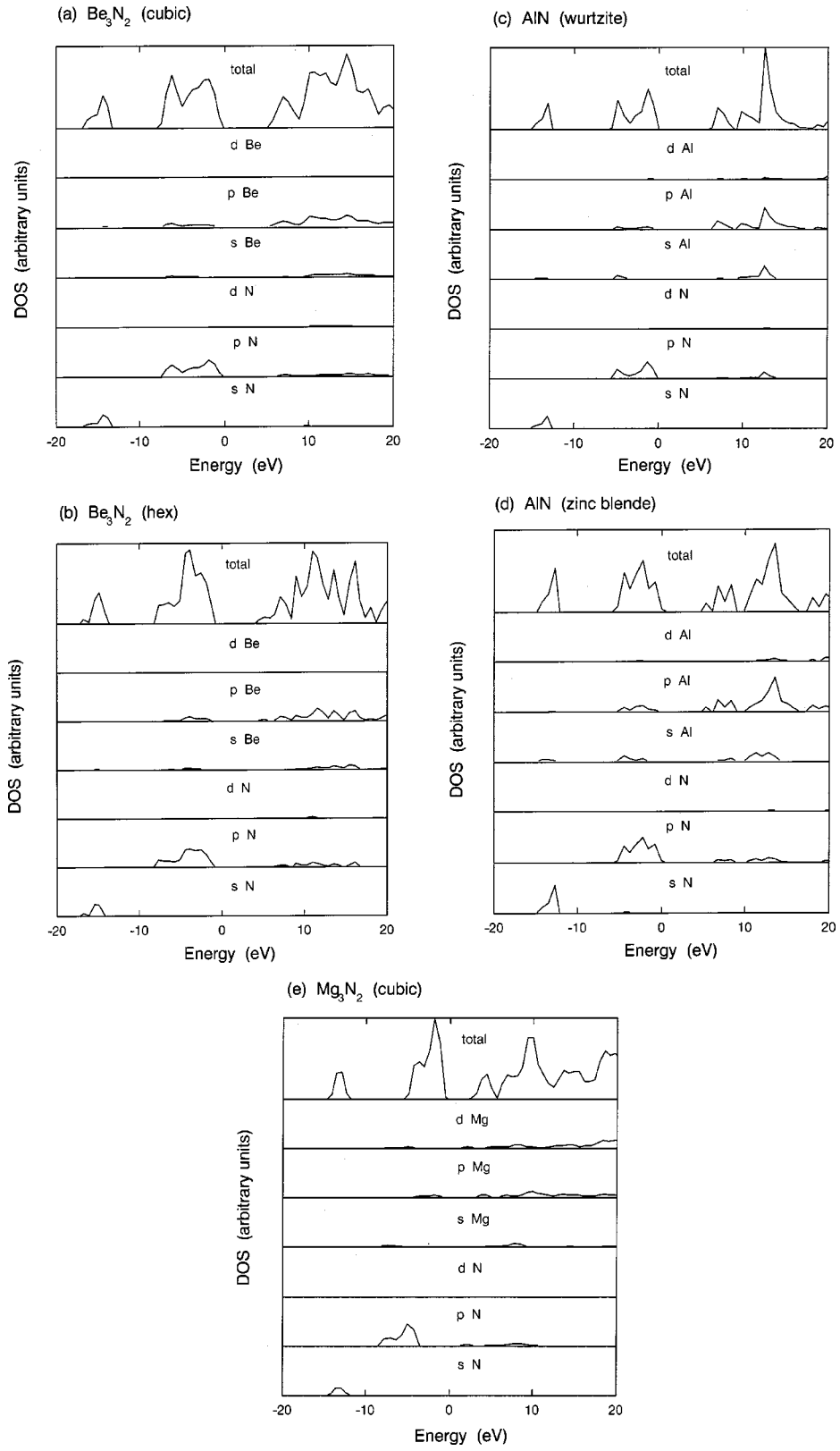

FIG. 4. Total and projected densities-of-states for different nitrides in this study. The energy zero is the valence-band top.

The electron charge density is calculated at the nodes of a one-dimensional array in a domain defined by the segment AB, where A and B represents the atoms.[20]

The charge difference density is defined as the difference between the superposition of atomic charge densities (periodic array of noninteracting atoms) minus the charge density of the same crystal structure.

We calculate the electron charge difference, to explore the degree of electronic charge transference in these materials along the Be-N, Al-N, and Mg-N bonds. The positive (nega-

TABLE IV. A Mulliken population analysis of the crystal wave functions from calculations performed with and without *d* orbitals. Distances and overlap populations are indicated for the differents bonds.

Compound	Atomic charge		Distance between neighbor atoms (Å)	Overlap population	
	6-21G	6-21G*		6-21G	6-21G*
α-Be_3N_2	8.051	7.993	1.731 N-Be	0.165	0.172
	8.038	7.978	1.744 N-Be	0.146	0.151
	3.306	3.346	1.750 N-Be	0.160	0.166
			1.761 N-Be	0.170	0.178
β-Be_3N_2	8.061	7.946	1.640 Be-N	0.185	0.202
	8.057	8.023	1.696 Be-N	0.204	0.211
	3.253	3.324	1.794 Be-N	0.148	0.153
	3.314	3.354			
AlN	8.256	8.249	1.881 Al-N	0.197	0.210
(wurtzite)	11.744	11.751	1.931 Al-N	0.187	0.206
AlN	8.241	8.224	1.890 Al-N	0.204	0.221
(zinc blende)	11.759	11.778			
Mg_3N_2	7.934	7.874	2.116 Mg-N	0.149	0.165
	7.925	7.880	2.133 Mg-N	0.119	0.168
	11.382	11.414	2.140 Mg-N	0.143	0.162
			2.154 Mg-N	0.164	0.153

tive) charge redistribution can be identified with electron transfer into bonding (antibonding) electronic states. We know that is not possible to obtain a quantitative value for the ionicity directly from the electron density.[44] The bond has a ionic component that can be identified with the charge transfer from the cation to the anion. On the other hand, the increase of charge density along the bond direction indicates strong covalent bonding.

In order to check the ionic behavior of the calculated compounds, we present the charge density difference along the representative bonds through the unit cell, as plotted in Fig. 5. Since the different bond lengths have been normalized to the same value, only a qualitative analysis of the shape of these curves is possible. The different ionicities of chemical bonds in AlN, Be_3N_2, and Mg_3N_2 can be already seen from representation of the valence-charge density along the bond direction as shown in Fig. 5. In comparison to the Be atoms in Be_3N_2, the probability to find valence electrons around the Al and Mg atoms in AlN and Mg_3N_2 is much lower. On the other hand the aluminum and magnesium (beryllium) atoms have more (minus) core electrons and a higher (lower) total density near the nuclear position, while the nitrogen atoms are more spread out with the larger number of valence electrons. A difference between the total electron density calculated with the 6-21G (no shown) and the 6-21G* basis set indicate that the effect of *d*-type polarization functions is a slightly accumulation of charge density in the bonding regions. Our calculated electron density in AlN is in good agreement with the results performed using plane-wave pseudopotencial approach.[29]

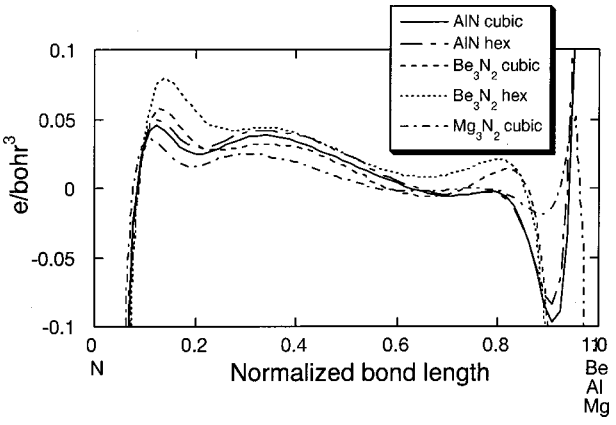

FIG. 5. Charge-density difference vs normalized bond length along the Be-N, Al-N, and Mg-N bonds.

In Table IV we present Mulliken population values. It can be observed that modified basis with *d*-type orbitals results in a small reduction of the ionicity of the structures, as can be observed in the minimum increase of the overlap population for the different bonds, and that the atomic charge is reduced by nitrogen atoms and it is increased by aluminum, magnesium, and beryllium atoms.

Mulliken population data per orbital shell of N, Al, Be, and Mg atoms is reported in Table V. Significant contributions are observed from the *d* shells of the Mg and Al atoms. This does not occur for Be and N where the effect of *d* shells is negligible. These *d* orbital effects have been found to be quite negligible for elements of the first and second row.

IV. CONCLUSIONS

This is the first *ab initio* determination of the electronic structure of the α-Be_3N_2 and Mg_3N_2 compounds.

It is observed that α-Be_3N_2 and AlN (wurtzite) presents a direct gap of 4.47 eV and 5.47 eV, respectively. When the calculations are performed with a 6-21G* basis set (that is including the *d*-type polarization functions), the gap 0.19 eV and 0.22 eV respectively. The α-Be_3N_2 has characteristics of a material with an important application for optoelectronic light-emitting devices.

TABLE V. Mulliken population data for the structures in the paper with basis set 6-21G* in atomic orbital shell.

	α-Be_3N_2		β-Be_3N_2		AlN (wurtzite)		AlN (zinc blende)		Mg_3N_2	
	Be	N	Be	N	Al	N	Al	N	Mg	N
2sp	1.266	2.165	1.251	2.134	7.896	2.190	7.899	2.194	7.922	2.114
3sp	0.052	3.825	0.175	3.886	1.479	4.058	1.518	4.030	0.628	3.766
4sp					0.223		0.202		0.510	
3d	0.030	0.007	0.029	0.007	0.152	0.004	0.155	0.004	0.361	0.002

The β-Be_3N_2, Mg_3N_2, and AlN (zinc-blende) structures show an indirect gap. According to our results, Mg_3N_2 could be considered a material with a direct gap, because the difference between the direct (2.26 eV) and indirect (2.25 eV) gap is very small.

Electronic distribution analysis at the atoms and at the bond regions between them, reveal a partial ionic character in all the nitrides of the present study. Our results show an increasing order of the ionicity: β-$Be_3N_2 \leqslant \alpha$-$Be_3N_2 \leqslant$ AlN (wurtzite) $\leqslant$ AlN (zinc blende) $< Mg_3N_2$.

ACKNOWLEDGMENTS

This work was supported by the Supercomputer Center DGSCA-UNAM and DGAPA Grant No. IN116898. M.G.M. acknowledges support from CONACYT for her graduate studies. We thank E. Aparicio for technical assistance.

*Author to whom correspondence should be addressed: Centro de Ciencias de la Materia Condensada UNAM, P.O. Box 439036, San Ysidro, California, 92143.

[1] H. Morkoc, S. Strite, G.B. Gao, M.E. Lin, B. Sverdlov, and M. Burns, J. Appl. Phys. **76**(3), 1363 (1994).

[2] V. Fiorentini, M. Methfessel, and M. Scheffler, Phys. Rev. B **47**, 13 353 (1993).

[3] S. Nakamura, Solid State Commun. **102**, 237 (1997).

[4] S. Nakamura, M. Senoh, S. Nagahama, N. Iwasa, T. Yamada, T. Matsushita, H. Kiyoku, and Y. Sugimoto, Jpn. J. Appl. Phys. **35**, L74 (1996).

[5] K. Miwa and A. Fukumoto, Phys. Rev. B **48**, 7897 (1993); N.E. Chrisiensen and I. Gorczyca, *ibid.* **47**, 4307 (1993); P.E. Van Camp, V.E. Van Dorem, and J.T. Devreese, *ibid.* **44**, 9036 (1991).

[6] W.R.L. Lambrecht, Mater. Res. Soc. Symp. Proc. **339**, 565 (1994).

[7] S. Strite and H. Morkoc, J. Vac. Sci. Technol. B **10**(4), 1237 (1992).

[8] Lev I. Berger, *Semiconductor Materials* (CRC Press, New York, 1997), p. 124.

[9] B.E. Douglas, D.H. McDaniel, and J.J. Alexander, *Concepts and Models of Inorganic Chemistry* (Wiley, New York, 1994).

[10] M.v. Stackelberg and R. Paulus, Z. Phys. Chem. Abt. B **22**, 305 (1933).

[11] P. Eckerlin and A. Rabenau, Z. Anorg. Allg. Chem. **304**, 208 (1960).

[12] G.T. Furukawa and M.L. Reilly, J. Res. Natl. Bur. Stand. **74A**, 617 (1970).

[13] T.B. Douglas and W.H. Payne, J. Res. Natl. Bur. Stand. **73A**, 471 (1969).

[14] D. Hall, G.E. Gurr, and G.A. Jeffrey, Z. Anorg. Allg. Chem. **369**, 108 (1969).

[15] R.W.G. Wyckoff, *The Structure of Crystals* (U. M. I., USA, 1991).

[16] *Crystal Data, Determinative Tables*, Department of Commerce, National Bureau of Standard, edited by Donnay, Inorganic Compounds Vol. 4, 1978.

[17] *Atlas of Crystal Structure Types for Intermetallic Phases*, edited by J.L.C. Daams, P. Villars, and J.H.N. van Vucht (ASM, Materials Park, 1991), Vol. 4.

[18] R. Dovesi, V.R. Saunders, C. Roetti, M. Causà, N.M. Harrison, R. Orlando, and E. Aprà, *CRYSTAL95 User's Manual* (University of Torino, Torino, 1996).

[19] J.P. Perdew and A. Zunger, Phys. Rev. B, **23**, 5048 (1981); A.D. Becke, Phys. Rev. A **38**, 3098 (1988).

[20] C. Pisani, R. Dovesi, and C. Roetti, *Hartree-Fock Ab-initio Treatment of Crystalline Systems*, Lecture Notes in Chemistry (Springer-Verlag, Heidelberg, 1988), Vol. 48.

[21] W.J. Here, T.R. Ditchfield, R.F. Stewart, and J.A. Pople, J. Chem. Phys. **52**, 2769 (1970).

[22] R. Poirier, R. Kari, and I.G. Csizmadia, *Handbook of Gaussian Basic Set a Compendium for Ab-Initio Molecular Orbital Calculations* (Elsevier, Amsterdam, 1985), Vol. 24.

[23] A. Reyes-Serrato, G. Soto, A. Gamietea, and M.H. Farias, J. Phys. Chem. Solids **59**, 743 (1998).

[24] E. Ruiz, S. Alvarez, and P. Alemany, Phys. Rev. B **49**, 7115 (1994).

[25] C. Pisani, R. Dovesi, and C. Roetti, *Quantum-Mechanical Ab-initio Calculation of the Properties of Crystalline Materials*, Lecture Notes in Chemistry (Springer-Verlag, Heidelberg, 1996), Vol. 67.

[26] F.D. Murnaghan, Proc. Natl. Acad. Sci. USA **20**, 244 (1944).

[27] W.H. Press, B.P. Flannery, S.A. Teukolsky, and W.T. Vetterling, *Numerical Recipes* (Cambridge University Press, New York, 1986).

[28] JCPDS-ICDD, International Centre for Difraction Data, PA.

[29] K. Karch and F. Bechstedt, Phys. Rev. B **56**, 7404 (1997).

[30] P.E. Van Camp, V.F. Van Doren, and J.T. Devreese, Phys. Rev. B **44**, 9056 (1991).

[31] M. Ueno, A. Onodera, O. Shimomura, and K. Takemura, Phys. Rev. B **45**, 10 123 (1992).

[32] L.E. McNeil, M. Grimsditch, and R.H. French, J. Am. Ceram. Soc. **76**, 1132 (1993).

[33] An-Ban Chen and Arden Sher, *Semiconductor Alloys* (Plenum Press, New York, 1997), p. 139.

[34] R. Orlando, C. Pisani, and C. Roetti, Phys. Rev. B **45**, 592 (1992).
[35] K.J. Chang and M.L. Cohen, Phys. Rev. B **30**, 4774 (1984).
[36] M. Gautier, J.P. Duraud, and C. Le Gressus, J. Appl. Phys. **61**, 574 (1987).
[37] C. Stampfl and C.G. Van de walle, Phys. Rev. B **59**, 5521 (1999).
[38] W.Y. Ching and B.N. Harmon, Phys. Rev. B **34**, 5305 (1986).
[39] I.N. Remediakis and K. Efthimios, Phys. Rev. B **59**, 5536 (1999).
[40] E. Rubio, J. Corkill, M. Cohen, E. Shirley, and S. Louie, Phys. Rev. B **48**, 11 810 (1993).
[41] J.C. Phillips, Rev. Mod. Phys. **42**, 317 (1970).
[42] R.S. Mulliken, J. Chem. Phys. **23**, 1833 (1955).
[43] W.J. Hehre, L. Radom, P.v.R. Schleyer, and J.A. Pople, *Ab-initio Molecular Orbital Theory* (Wiley, New York, 1986).
[44] N.E. Christensen, S. Satpathy, and Z. Pawlowska, Phys. Rev. B **36**, 1032 (1987).